Fluid Distribution in Packed Beds. Part 2. Experimental and Phenomenological Assessment of Distributor and Packing Interactions

Giulia Bozzano,* Mario Dente, and Flavio Manenti

Politecnico di Milano, Dipartimento di Chimica, Materiali e Ingegneria Chimica "Giulio Natta" Piazza Leonardo da Vinci 32, 20133 Milano, Italy

Paola Corna and Fabio Masserdotti

SIAD Macchine Impianti, Via San Bernardino 92, 24126 Bergamo, Italy

1. INTRODUCTION

The use of well-designed distributors, the knowledge and deep understanding of their behavior under conventional and nonconventional operating conditions, and their interactions with the packing are all key points to exploit the potentialities of the structured packing and, therefore, of the whole unit operation. The literature offers a wide set of works aimed at studying and optimizing the packing and the liquid distributors without deeply analyzing their interactions. Several authors[1−4] devoted their papers to the description and quantification of liquid maldistribution in packed systems. Other authors have demonstrated the masking effect of oversized equipment on the gas and liquid maldistributions,[5,6] also quantifying the increase with the height equivalent theoretical plate (HETP). The maldistribution effect is different for random and structured packing.

With random packing, a traditional method to analyze liquid maldistribution is based on the use of specially designed collecting vessel, installed below the packing bed to collect liquid falling down.[5] It is frequently measured by adopting a maldistribution factor, Mf, originally defined by Hoek and co-workers.[6,7] Interesting experimental apparatus and techniques have been proposed in the literature by Ter Veer et al.,[8] Pizzo et al.,[9] Kouri and Sohlo,[10,11] and Ibrahim.[12] Mechanistic[13] and statistical[5] models of liquid distribution in a packing wetted by a multipoint distributor have been proposed. A good review on the existing models is also provided by Sun et al.,[14] including models based on the concept of random walk[7,15−19] and models with diffusion terms.[7,17−19]

In case of structured packing, if a good distribution of the liquid and gas flows is realized, it is maintained for a longer bed height than in the case of random packing. In comparison with random packing, structured packing requires a better inlet distribution of gas and liquid. Also, in this case, it is important to consider that different packing configurations could lead to different maldistribution effects. Due to this reason, Stikkelmann et al.[20] have studied the gas and liquid distribution in different types of structured packing, and Edwards and co-workers[21] carried out a characterization of the maldistribution of liquid and gas flows by changing the distributor. More recently, other authors[22,23] analyzed the behavior of different high capacity packings varying also the gas and liquid flows and the packing height.

Regarding the gas inlet flow, in general, the commercially available liquid distributors, specifically designed for structured packing columns, are based on an elementary concept accepted for several decades for random packings.[3] That is, the gas does not need additional redistribution, because the bed pressure drop acts by itself as flow distributor.

Spiegel[24] started to analyze the relation between the outflow of the distributor and the wetting condition of the packing immediately underneath it, which was then studied by other authors also in different fields[25,26] (e.g., trickle-bed reactors) and is also the aim of the present paper. It is now clear how gas and liquid mutual distribution plays a fundamental role in the efficient operation of a packed column. Poor distributions reduce the effective wet packing and, from a practical point of view, they lead to reduced performances due to poor gas−liquid contact efficiency and to reduce effective interfacial area

Received: July 6, 2013
Revised: November 28, 2013
Accepted: January 21, 2014
Published: January 21, 2014

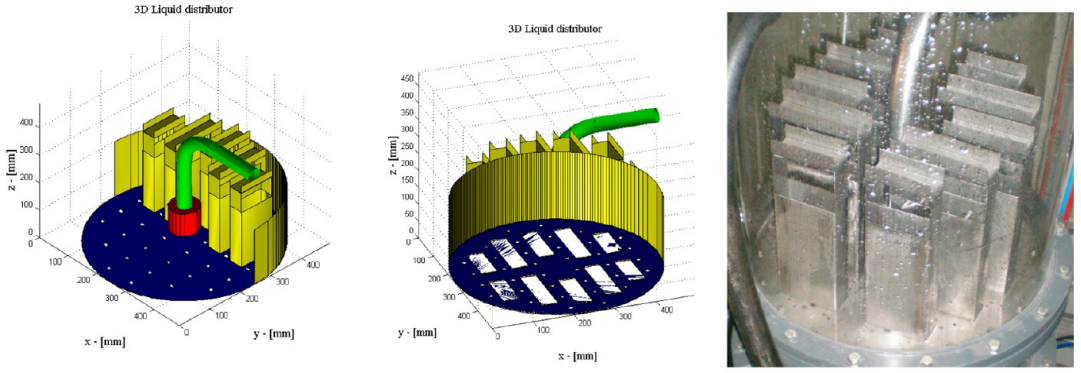

Figure 1. Sketch of the top (a) and bottom (b) of the gravity distributor, picture of the installed distributor in operation (c).

for mass transfer, imposing a higher HETP to match the expected performances.[27−29]

A companion paper,[30] which this work is strictly related to, reports in a more extended way a review of the available literature.

The literature analysis evidences the necessity of studying in a deeper way the influences of the interactions between the liquid distributor and the underlying packing. So the attention is here focused on studying these aspects by means of an extended experimentation.

The literature provides some guidelines or procedures to design and set up in practice a pilot plant. Many authors, however, often provide the specifications of their laboratory or pilot plants without mentioning the reasons behind their selections, whereas other authors discuss optimal experimental design by assuming that their experimental instrumentation is the most appropriate one to perform optimal analyses. Whenever the plant is nonoptimal for investigating the fluid-dynamics or the chemical-physical phenomena, even an optimal design of experiments can be useless. Especially for this reason, it is necessary, first, to provide the path for the reasonable design and construction of a pilot plant. For the specific case of interest, an air/water system with structured packing and liquid distribution is discussed.

According to Spekuljak and Monella,[4] a well-designed liquid distributor has to fulfill the following requirements: the largest number of drip points, maximum homogeneity among flow rates of the different drip points, operating flexibility, avoiding formation of drops and mist, avoiding splashing, avoiding the merging of single jets generated by the distributor, maximizing the gas flow cross-section, allowing the gases to disengage, avoiding scale or dirt deposition, being mechanically robust, being easy to clean, and having reasonable cost compared to that of the column.

The operation of a distillation column is strictly related to its design. Each column has accurate operational parameters that cannot be overcome to preserve the stability or the good distribution of fluids and, therefore, the efficiency. In spite of the usual industrial narrow operating conditions, the pilot plant has to be designed to investigate the largest possible operating region. Thus, a flexible configuration for the internal disposition of distributor and packing must be allowed.

It has been considered interesting to design the column to study the following cases:

1. Minimum load: the optimal operating condition is given by the operational capacity of the liquid distributor to create falling jets with certain ideal features to wet the packing effectively with the minimum water flow rate. Such a case is called the turndown condition.

2. Maximum load: this corresponds to the maximum liquid flow that can be distributed by the liquid distributor. Such a condition is obtained by supplying a certain liquid flow rate that, subject to the pressure drops due to the gas flow rate, fills the liquid distributor up to the weirs of the risers designed for the air flow. This case is defined as the distributor overcapacity.

3. Intermediate load: this is the typical operational condition of the system.

4. Packing loading: an experimental campaign will be devoted to analyzing in detail the efficiency of the structured packing under the maximum theoretical conditions of mass transfer by means of appropriate water and air flow rates and the use of appropriate mathematical models for both prevision and verification purposes.[31]

This paper is dedicated to the experimental campaign and phenomenological discussion of the typical operational loads (minimum, intermediate, and maximum loads) and to the investigation of nonconventional conditions.

2. PILOT PLANT DESIGN AND CONSTRUCTION

In the case of packed unit operations and fluid distributors, the most appealing system for experimental studies is the air/water column,[12,20,23,28,29,32] since it is simpler and safer with respect to other systems that involve different chemical species. This system, of course, implies a low wettability of the stainless steel surface of the packing, so that water is falling as rivulets. However, it will be shown that good water distribution is obtained in the proposed system. Probably the interaction of the liquid with the air should demonstrate a different behavior with a more hydrocarbon like liquid having a lower surface tension, so that a specific experimental campaign would be interesting and could be the object of a further investigation.

Due to the large number of experiments performed for studying the system (184 tests), it has been decided to adopt only one type of liquid distributor, one type of structured packing, and one gas−liquid system.

2.1. Liquid Distributor. According to the features above, a gravity distributor (Figure 1) has been selected among all the kinds of commercial liquid distributors. The distributor desk is sieved with drip points (5 mm diameter) in rectangular grids. Special covers are supplied over the air risers in order to intercept the entrained drops. The risers installed on the distributor deck have a total cross area of 30% of the overall

distributor. Their height is 20 cm. The distributor has been installed to allow the investigation (1) of the twist angle between the layers of the structured packing and the lines of drip points, (2) of the distance between the distributor and the packing below, and (3) of the effect of possible fouling (the possibility to close 50% of the drip points has been foreseen).

2.2. Structured Packing. A Mellapak 250.Y was selected (259 m^2/m^3 surface area, 98.3% void fraction, 210 mm pack height, wiper bands and internal paths to improve the internal distribution of liquid). Even if the packing consists of a single structured block, in the present study a hold down and a hold up were inserted in order to simulate at best the operating conditions of the real packed columns and to provide a comprehensive phenomenological description.

2.3. Liquid Collector. To measure the liquid distribution of the water flowing out of the packed bed, a liquid collector with nine evenly sized vessels, which are separated from each other, is placed at the bottom of the column (Figure 2). Each one of these containers is connected to a pipe that removes the water and allows one to measure the water flow rate of each vessel. The open area is necessary in order to allow the air to pass from the bottom of the column where the gas inlet distributor is installed.

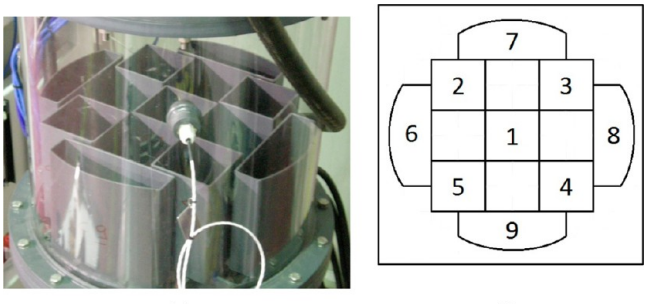

Figure 2. Picture of the containers for liquid collection under the packing (a) and sketch of the collecting system (b).

2.4. Gas Distributor. Because of the small column diameter, a toroid shape has been selected for the gas distributor. The air enters through a large flange (1), impacts toward the wall (2), and is addressed to the bottom (3). When the torus borderline is reached, the air changes direction (4) and starts to move toward the vessels and the column top (5). The qualitative gas streamlines are represented by the arrows in Figure 3.

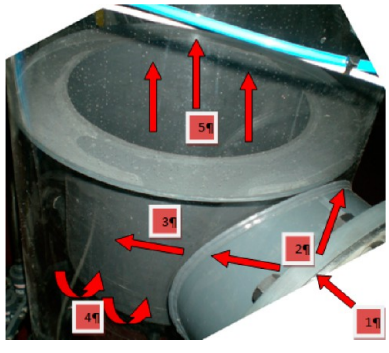

Figure 3. Gas distributor and qualitative streamlines.

2.5. Tray with Risers and Demister. Under certain operating conditions, liquid entrainment occurs. For evaluating the relevance of this effect, a tray with risers is installed to collect the entrained liquid. This tray is placed close to the top of the column, just under the demister. Eventually, some liquid can achieve the demister, which carries out the final separation between gas and liquid, allowing the gas to leave the column and the liquid to fall down to the underlying tray. Only in very extreme situations, out of the usual industrial operating conditions, can liquid overcome the demister and exit from the column top.

2.6. Column Vessel. Given the purpose of the pilot plant, the column is realized with a transparent vessel in order to allow visual observations of the fluid-dynamic phenomena. The selected material is poly methyl methacrylate. A picture of the column and a sketch of the pilot plant are reported in Figure 4. The column diameter is 490 mm (the plant was built at SIAD MACCHINE IMPIANTI, Italy).

A programmable logic controller (Siemens PLC) has been provided to collect all the experimental data as well as to start up and shut down the units in a safe mode.

3. EXPERIMENTAL PROCEDURE

An ad hoc startup procedure was adopted to start the data acquisition. It was split into two phases: the prestartup and the startup. Whenever the water of the previous test was completely changed, the prestartup was needed, because the plant operates like an air filter for the soot and the solid particles of the air. The water was then completely replaced after 8 h of operations. The startup procedure has been accurately standardized in order to reach a good reproducibility of the results. Of course, after the startup phase, 10 to 40 min were necessary for achieving the steady-state conditions.

To better identify the tests among the wide set of the available data, the following notation is adopted containing four groups of information. The first one relates to the number of active drip points of the distributor (as in Figure 5). The second one refers to the adopted distributor to packing distance (as in Figure 6). The third one gives the twist angle (0°, 45°, and 90° as in Figure 7), and the last one indicates the gas (according to Table 1) and liquid flow rate (according to Table 2, where it is possible to observe that GE3 allows lower flow rates). For instance, GE1.D2.0.F.3.2 indicates, respectively, 36 active drip points (GE1), the distance, D2 = 26 cm, between packing and liquid distributor, the twist angle 0°, the air flow (F) rate (3 = 2000 kg/h), and the water flow rate (2 = 1000 kg/h).

To generalize experimental data, the specific flow rates are used. For the specific gas flow rate, F_s, largely adopted in the column design, is used (it accounts for the column total cross section, but also the gas density):

$$F_s = v_{gas}\sqrt{\rho_{gas}} \quad (1)$$

where v_{gas} is gas velocity = volumetric flow rate/column total cross section and ρ_{gas} is gas density.

4. EXPERIMENTAL DATA AND DISCUSSION

The behavior of the liquid level in the distributor is presented in Figure 8 as a function of the specific gas flow rate F_s and for different specific liquid flow rates. As expected, the higher the water load, the higher the liquid level.[33] It is easy to observe that the gas flow rate plays a significant role in the liquid level;

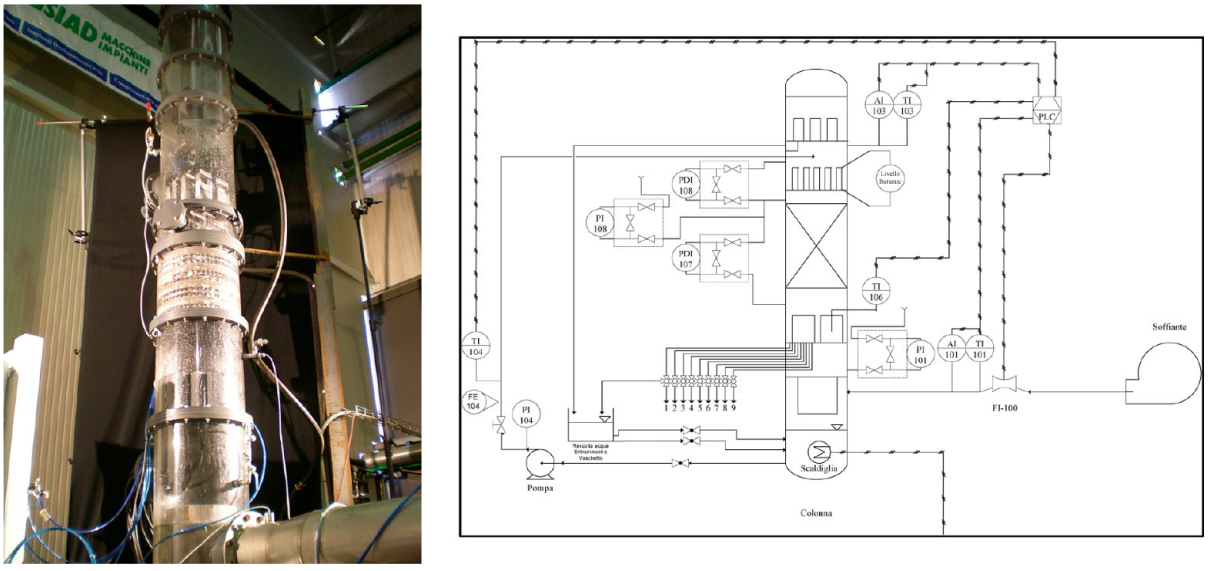

Figure 4. The column and a sketch of the pilot plant.

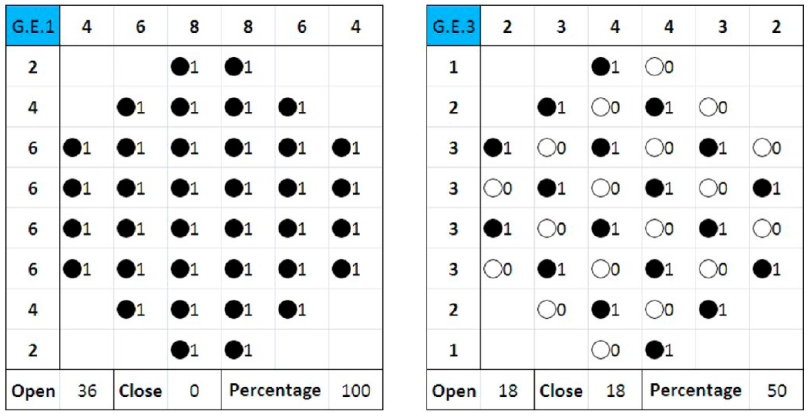

G.E.1	4	6	8	8	6	4
2			●1	●1		
4		●1	●1	●1	●1	
6	●1	●1	●1	●1	●1	●1
6	●1	●1	●1	●1	●1	●1
6	●1	●1	●1	●1	●1	●1
6	●1	●1	●1	●1	●1	●1
4		●1	●1	●1	●1	
2			●1	●1		
Open	36	Close	0	Percentage		100

G.E.3	2	3	4	4	3	2
1			●1	○0		
2		●1	○0	●1	○0	
3	●1	○0	●1	○0	●1	○0
3	○0	●1	○0	●1	○0	●1
3	●1	○0	●1	○0	●1	○0
3	○0	●1	○0	●1	○0	●1
2		○0	●1	○0	●1	
1			○0	●1		
Open	18	Close	18	Percentage		50

Figure 5. Outflow geometries (black drip point means open/active).

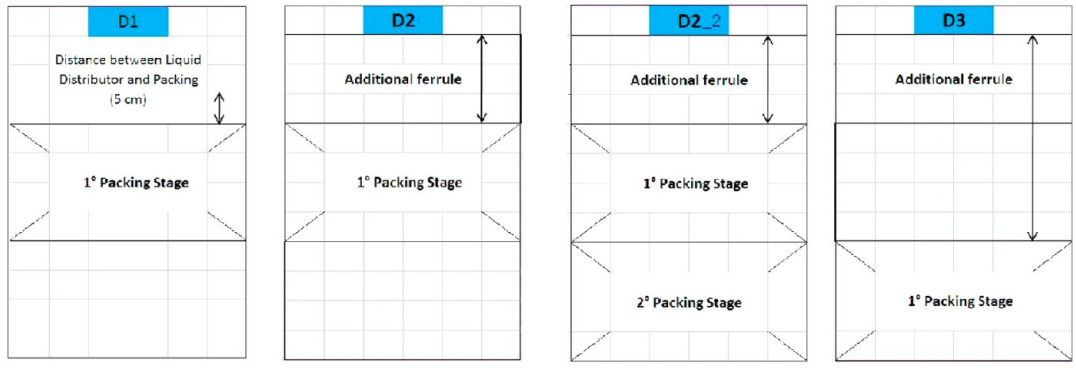

Figure 6. Distance between the structured packing and the distributor deck: 5 cm (D1), 26 cm (D2), and 50 cm (D3).

in fact, higher loads lead to higher pressure drops across the distributor deck, of course at the expense of liquid level. The lines corresponding to the lowest water loads have a linear trend; on the contrary, as the liquid load increases, the gas pressure drops on the distributor assume an about quadratic trend. This is clear for the intermediate loads; actually, the effect of the water flow rate is more evident because of the higher liquid level. The dotted line corresponding to 200 mm represents the maximum liquid level. For the higher liquid load, F_s is limited in range.

Figure 9 shows the effect of the gas load on the pressure drops. It can be observed that, with small air flow rates, the pressure drops are almost the same for all the liquid loads. On the other hand, when the air load increases, the effect is not anymore negligible. Analyzing first of all the reference test, where the trend is related only to the gas flow rate (no liquid load), it is possible to quantify the energy dissipated by the air

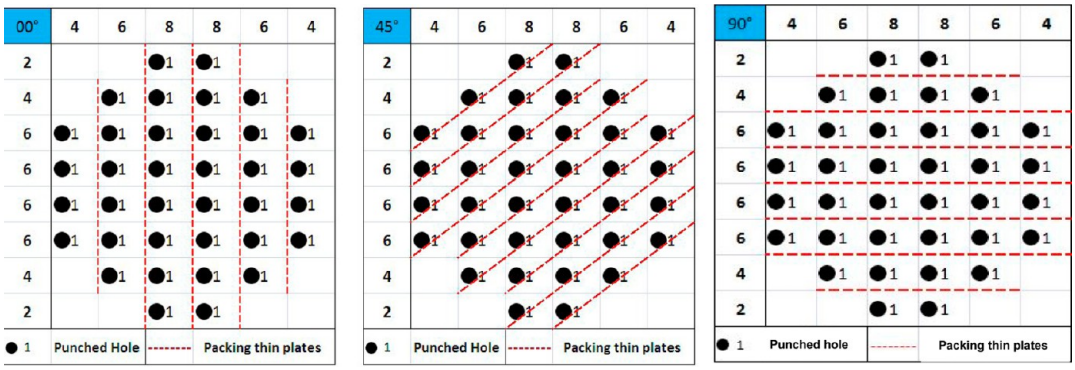

Figure 7. Twist angles.

Table 1. Gas Flow Rates (kg/h)

1	2	3	4	5	SL
1100	1500	2000	2300	2700	4500

Table 2. Liquid Flow Rates (kg/h)

	1	2	3	4	5	6
GE1 (36 drip points)	600	1000	1400	2000	2600	3500
GE3 (18 drip points)	600	1000	1400	1800	2000	

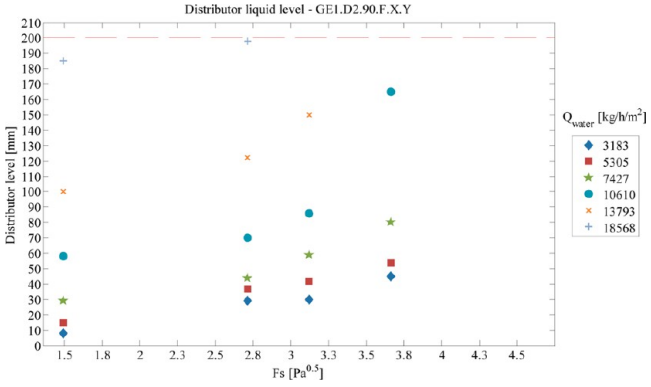

Figure 8. Liquid level in the distributor as a function of F_s.

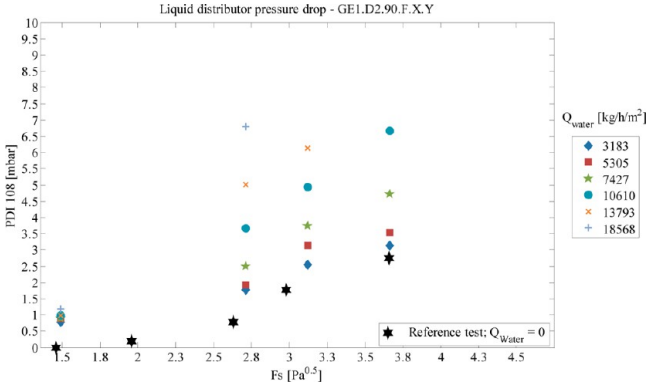

Figure 9. Pressure drops on the liquid distributor.

passing through the risers. By introducing the water in the countercurrent, the pressure drops monotonically increase, but the deviation is quite small for low liquid loads, since the profiles are almost parallel. The larger flow rates (>10 000 kg/h/m^2) generate a pressure increase immediately below the distributor deck, with a subsequent increase of the pressure drops. This is mainly related to the adherence of the air to the falling jets generating a detrimental effect over the air movement toward the risers.

Figure 10 reports the corresponding pressure drops of the structured packing. Also in this case, they are strictly related to

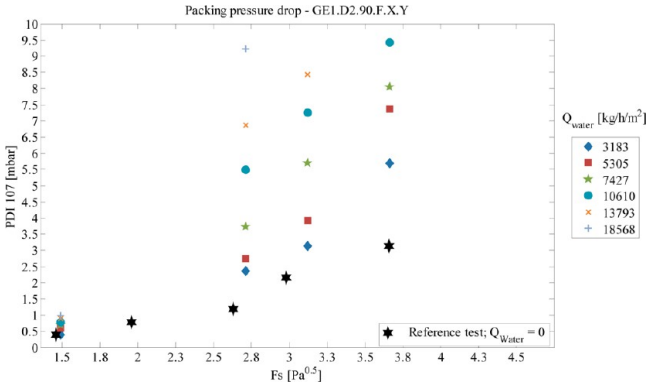

Figure 10. Load profile on the structured packing.

the gas load. This is due to the high void fraction of the Mellapak 250.Y, which allows a good internal distribution while enough space is still available for the small gas flow rate supplied. When the liquid flow rate increases, the cross-section of the channels is progressively reduced and the profile of the pressure drops assumes a nonlinear trend. When the gas flow rate is sufficiently large, the so-called loading condition is approached. It is well-known that near the loading conditions, the pressure profile shows a sudden, exponential, increase.

The amount of liquid entrained by the gas flow rate is illustrated in Figure 11. It is possible to highlight several important aspects to clarify the quasi-quadratic profiles of these results:

1. A low liquid flow rate leads maldistributions and instabilities of the falling film; moreover there is an increase of the droplets generated and entrained. An inversion of the trend of the entrainment phenomenon, which is more apparent with smaller air flow rates, can be observed. This happens since the smaller the air flow rate, the lower the liquid level on the distributor deck for the reduced pressure drops and, hence, the more significant the instability of the falling jets (with droplet generation). Indeed, the higher the gas flow rate, the higher the pressure drop on the distributor and the higher the liquid level. This unavoidably leads to higher outflow velocities and more stable jets of liquid (reduced entrainment and weeping problems).

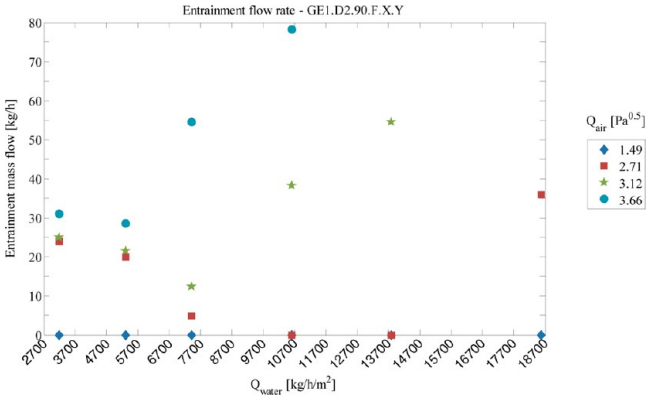

Figure 11. Results of entrainment tests.

2. At large liquid flow rates, the entrainment becomes more and more significant since the structured packing is approaching the loading, and then flooding, conditions.

3. At average liquid flow rates, the entrainment is negligible, since the liquid flow is enough to preserve the liquid film stability and continuity. Moreover, the column operates under or close to the loading conditions so that the entrained liquid is surely less than in case 2.

4. Of course at low gas flow rates, there is not relevant entrainment independently of the liquid load since the gas flux is too weak to raise the liquid droplets up to the distributor.

4.1. Hydraulic Tests. *4.1.1. Analysis of the Liquid Distribution on the Packing.* A proper liquid distribution coupled together with the effectiveness of the structured packing leads to the best conditions for mass transfer and the highest efficiency. From a hydraulic viewpoint, the effects of the twist angle, the distance between the distributor and the packing, and the different geometrical arrangement of drip points can be evaluated by maintaining the packing configuration and only modifying the geometrical parameters of the distributor. Some experiments have been addressed to define the optimal installation of the distributor. The test was based on the acquisition of the data related to the liquid distribution underneath the packing using the specific collectors. Hereinafter, the liquid distribution below the packing is reported for different geometries. The wetting profiles of the packing are evaluated by accounting for gas flow rate, liquid flow rate, and entrainment effect. Each figure is coupled with a table reporting the experimental flow rates of each vessel and the evaluation of the Maldistribution Factor (Mf) that is here defined, accordingly with Marcandelli et al.,[34] as

$$\mathrm{Mf} = \sqrt{\frac{1}{N\cdot(N-1)}\sum_{1}^{9}{}_{i}\left(\frac{Q_i - \bar{Q}}{Q_i}\right)^2} \qquad (2)$$

where N is the number of experimental points, Q_i the volumetric flow rate of each vessel, and $\bar{Q}$ the averaged flow rate of the nine vessels.

The figures have been obtained by using the measured flow rate in each vessel, the column inlet flow rate, and the entrainment flow rate. The reported profiles have been obtained starting from the massive flow rate of each vessel. By assigning coordinate x,y to the center of each vessel (see Table 3), the corresponding z coordinate indicates the massive flow rate. In order to obtain a smoother profile and avoid jumping, among vessel 1, 2, 5, and 6, a point having the average massive flow rate of the four considered vessels is reported. The same has been done for the vessels 1, 2, 3, and 7; 1, 3, 4, and 8; and 1, 4, 5, and 9. Starting from these points, an interpolation is performed together with a normalization to the total massive flow rate (including entrainment).

Figure 12 refers to moderate air and water flow rates, i.e., under "ideal" conditions. A sufficiently uniform distribution of the liquid below the packed bed means that this configuration has a very good hydraulic behavior. If the liquid flow rate is increased, at a constant gas flow rate, the wetting profile does not change significantly, except for the liquid level, as expected (Figure 13). Conversely, keeping a constant liquid flow rate and increasing the gas flow rate, the liquid distribution starts deviating from the ideal profile, as shown in Figure 14. Apparently, the profile seems to maintain a uniform distribution on the whole cross-section, but the measured entrainment effect is relevant. Actually, looking at the two-dimensional view, it is possible to see that the profile is below the ideal wetting condition (horizontal line in the two-dimensional view and disk in the three-dimensional view) because a large part of the liquid is entrained and lost at the top of the column. The crossed plane represents the level connected to an ideal wetting of the package.

The worst distribution condition is obtained with a large gas flow rate combined with a large liquid flow rate (Figure 15). This test shows a profile that is significantly lower than the ideal distribution (Mf = 0.105), indicating that yet a relevant portion of the liquid is entrained and lost. Moreover, the distribution is clearly heterogeneous since the liquid profile presents a kind of crown effect, which is due to two interacting causes:

- At high gas flow rates, the velocity profile is not uniform on the cross-section. In fact, a bell-like profile is to be expected below the packing where the lower peripheral velocities are due to the friction with the column vessel and flange that supports the internal devices. Although it has been tried to minimize the effect, it results in a stronger frictional force with respect to the center of the column.
- Because of the previous phenomenon, the falling liquid prefers to flow down in the peripheral regions; the wiper bands try to oppose to this behavior, leading to the crown effect.

In addition, the larger liquid flux in the peripheral zones further amplifies the crown effect on the distribution, forcing the gas toward the central region of the packing.

4.1.2. Effect of the Outflow Geometry. Two different numbers of active drip points have been adopted: 36 for all the runs GE1 and 18 only for the runs GE3. Moreover, three different twist angles and three distributor-to-packing distances have been adopted. The geometry influences the liquid level

Table 3. Coordinates of the Center of the Vessels

vessel no.	1	2	3	4	5	6	7	8	9
x [mm]	245	135	355	355	355	0	245	490	245
y [mm]	245	135	135	355	135	245	490	245	0

GE3.D3.00.F1.2

Vessel n°	m³/h	Av. m³/h
1	0.042	0.057
2	0.055	
3	0.065	**Mf**
4	0.065	**0.058**
5	0.072	
6	0.055	
7	0.065	
8	0.048	
9	0.048	

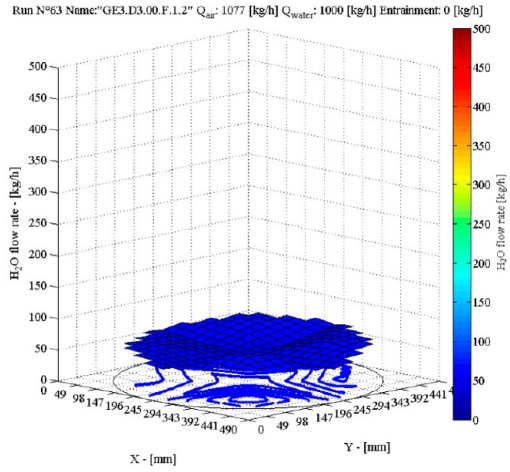

Figure 12. GE3.D3.00.F.1.2, liquid distribution below the packing.

GE3.D3.00.F1.4

Vessel n°	m³/h	Av. m³/h
1	0.095	0.11
2	0.078	
3	0.138	**Mf**
4	0.120	**0.055**
5	0.095	
6	0.112	
7	0.120	
8	0.120	
9	0.112	

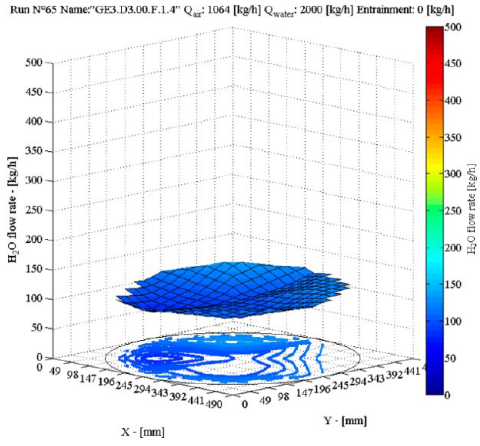

Figure 13. GE3.D3.00.F.1.4, liquid distribution below the packing.

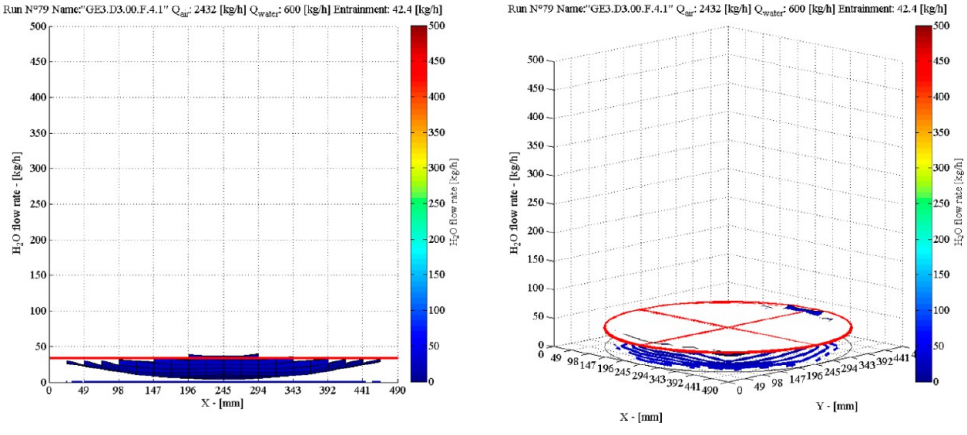

Figure 14. GE3.D3.00.F.4.1, liquid distribution below the packing with high gas flow rates and low liquid flow rates.

over the distributor deck, the pressure drops of the distributor and of the packing as well, the entrainment, and the liquid distribution below the packing. Figures 16–21 report the results of these experiments.

Specifically, Figure 16 shows the effect of the geometry on the liquid level over the distributor. Note that for low liquid flow rates, the level is more or less the same, although the level for GE3 is more influenced when the gas flow progressively increases. With large liquid flow rates and small gas flow rates, of course, it can be observed that a flow of GE3 is equal to about half a flow of the GE1.

This simple consideration is not any more valid as the gas flow rate increases; the deviation becomes more relevant when $F_s > 2.8$. Figure 16 shows that in case of fouling of the holes of the distributor, the liquid flow rates have to be reduced for high gas flow rate in order to avoid reaching the distributor overcapacity.

GE3.D3.00.F4.4

Vessel n°	m³/h	Av. m³/h
1	0.021	0.084
2	0.077	
3	0.080	**Mf**
4	0.090	**0.105**
5	0.086	
6	0.100	
7	0.110	
8	0.106	
9	0.088	

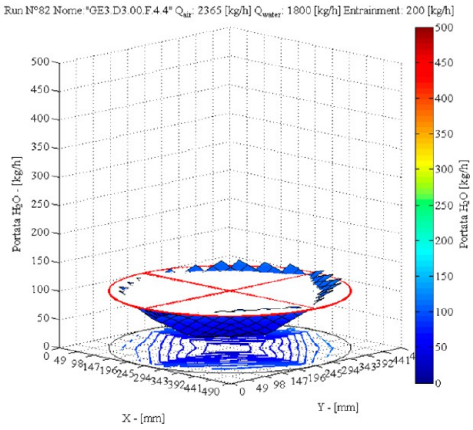

Figure 15. GE3.D3.00.F.4.4, liquid distribution below the packing for high liquid and gas flow rates.

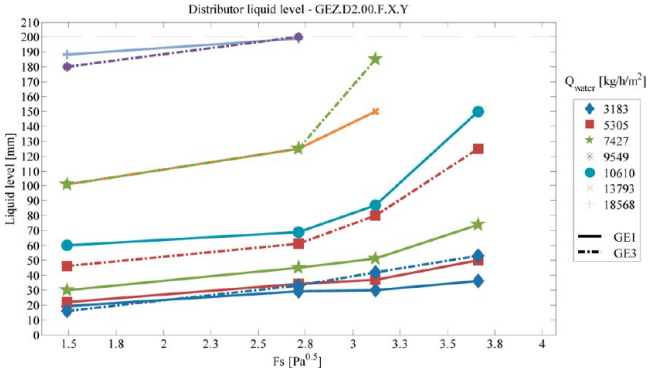

Figure 16. GE1.D2.00.F.x_axis.y_axis versus GE3.D2.00.F.x_axis.y_axis, liquid level on the distributor.

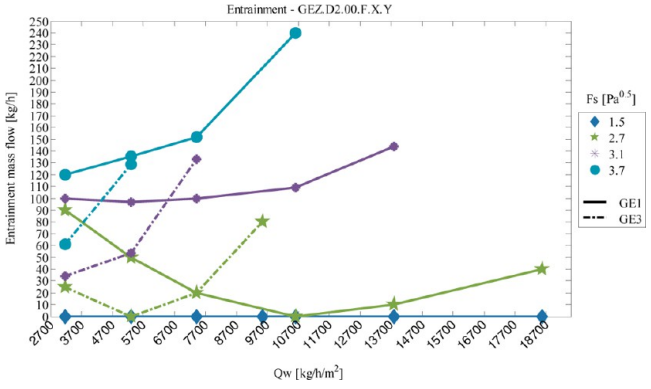

Figure 17. GE1.D2.00.F.x_axis.y_axis versus GE3.D2.00.F.x_axis.y_axis, entrainment flow rate.

Figure 17 shows the behavior of the liquid entrainment corresponding to the selected geometries. A first, obvious, consideration is that no entrainment is present at low F_s. Looking at the two curves obtained with different geometries under the same operating conditions, it is possible to observe a dependence on the liquid flow rate, which is more or less close to the loading condition of the packing, as well as on the outflow velocity of the liquid and its possible instability. GE3 configuration, having to distribute the same quantity of liquid with half the number of drip points, generates splashing of the liquid jet because of its increased velocity. So the conclusion rising from Figure 17 is that in the case of severe distributor drip points fouling, even if uniformly distributed as in our case, the entrainment increases with a loss in efficiency of the system.

The liquid distribution below the packing corresponding to the two configurations is reported in Figures 18–20. The comparison is made taking into account the velocity outflow from the drip points of the distributor that has to be the same. So for the GE1 configuration, the liquid flow rate is about double that for the configuration GE3. Under this point of observation, it is possible to observe that the two configurations show the same order of magnitude of maldistribution both for low and high liquid flow rates. In the GE1 configuration, a tendency to dislocation of the liquid toward the column wall because of the higher liquid hold-up on the packing is evident.

4.1.3. Effect of the Twist Angle. To assess the effects of the twist angles, the geometry GE3.D2.zz.F.x.y with zz = 0°, 45°, and 90° and x and y as in Tables 1 and 2 has been tested. Figure 21 shows that the effect of the twist angle on the liquid level is practically negligible. However, in general the twist angle of 0° shows the lowest holdup. The twist angle 0° induces also reduced pressure drops on the distributor. Clearly, this is due to the disposition of the risers (rather than to the position of the drip points); in fact, the risers have a rectangular cross-section, and whenever the longer side is parallel to packing layers, the gas flow can enter the risers without significantly changing its path.

Figure 22 includes two air–water flow rate configurations with the three selected twist angles. It is possible to observe that for the lower air flow rate (about one-half of the liquid flow rate) the liquid is well distributed in all of the configurations. When the air flow rate is much higher than the liquid flow rate, maldistribution is the same in all the situations so that it is possible to affirm that the twist angle has no particular influence in this system of the liquid distribution, while it has an impact on the liquid level of the distributor.

4.1.4. Effect of the Distributor to Packing Distance. The selected geometry for the sensitivity analysis of the (distributor-packing) distance is the GE1.Dz.90.F.x.y with z = 1, 2, and 3 and x and y as in Tables 1 and 2. The adopted distances are 5 cm (D1), 26 cm (D2), and 50 cm (D3). D2 and D3 have equal trends. Then the effects due to the distances D1 and D2 are provided in the following.

From Figure 23, it is possible to observe that at the lowest liquid loads the liquid level is, in practice, independent of the distance and the gas loads. However, a relevant variation in the slope of the curves appears for the distance D1 when the liquid

GE1.D2.90.F.1.1

Vessel n°	m³/h	Av. m³/h
1	0.036	0.103
2	0.048	
3	0.053	**Mf**
4	0.055	**0.153**
5	0.060	
6	0.160	
7	0.180	
8	0.170	
9	0.170	

GE3.D2.90.F.1.1

Vessel n°	m³/h	Av. m³/h
1	0.011	0.033
2	0.033	
3	0.033	**Mf**
4	0.034	**0.09**
5	0.034	
6	0.036	
7	0.042	
8	0.036	
9	0.040	

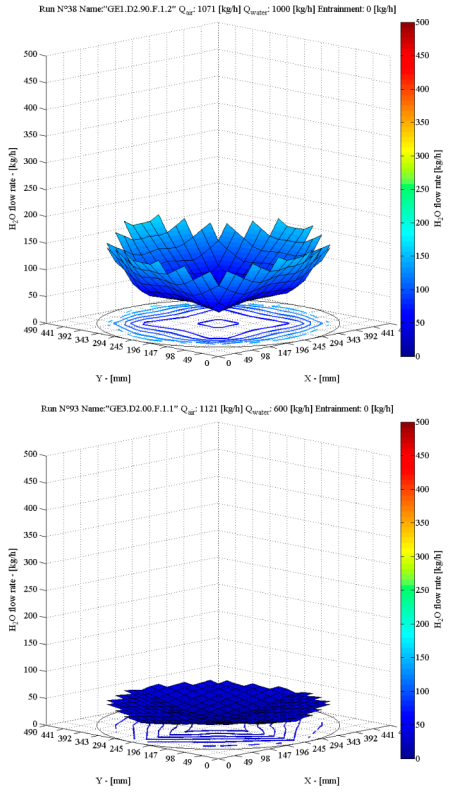

Figure 18. Liquid distribution below the packing with reduced water and air flow rate and different plugging of drip points.

GE1.D2.90.F.3.3

Vessel n°	m³/h	Av. m³/h
1	0.030	0.075
2	0.040	
3	0.048	**Mf**
4	0.041	**0.186**
5	0.041	
6	0.109	
7	0.124	
8	0.116	
9	0.124	

GE3.D2.90.F.3.1

Vessel n°	m³/h	Av. m³/h
1	0.019	0.034
2	0.019	
3	0.026	**Mf**
4	0.026	**0.143**
5	0.022	
6	0.055	
7	0.051	
8	0.045	
9	0.045	

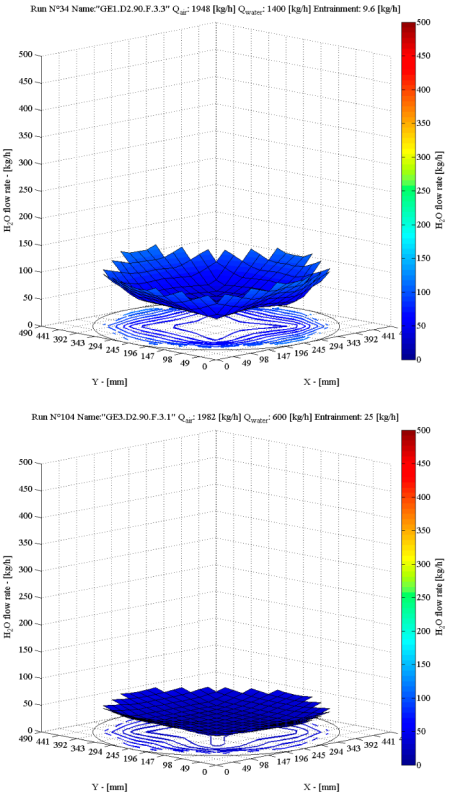

Figure 19. Liquid distribution below the packing with reduced water flow rate and different plugging of drip points.

flow rates rise. This phenomenon takes place at relatively low F_s for the larger liquid loads. The consequence is the impossibility to obtain data for $F_s > 2$ due to the distributor overflow. This effect depends on the pressure drops on the distributor (Figure 24). Actually, when the pressure drops have a relevant increase, the slope of the liquid level dramatically changes. Qualitatively speaking, particularly for the lowest distance D1, the gas streamlines are forced to anticipate their deflection already into

GE1.D2.90.F.4.4

Vessel n°	m³/h	Av. m³/h
1	0.055	0.084
2	0.067	
3	0.064	**Mf**
4	0.063	**0.084**
5	0.065	
6	0.100	
7	0.097	
8	0.106	
9	0.079	

GE3.D2.90.F.3.3

Vessel n°	m³/h	Av. m³/h
1	0.112	0.089
2	0.086	
3	0.090	**Mf**
4	0.082	**0.040**
5	0.086	
6	0.086	
7	0.082	
8	0.075	
9	0.089	

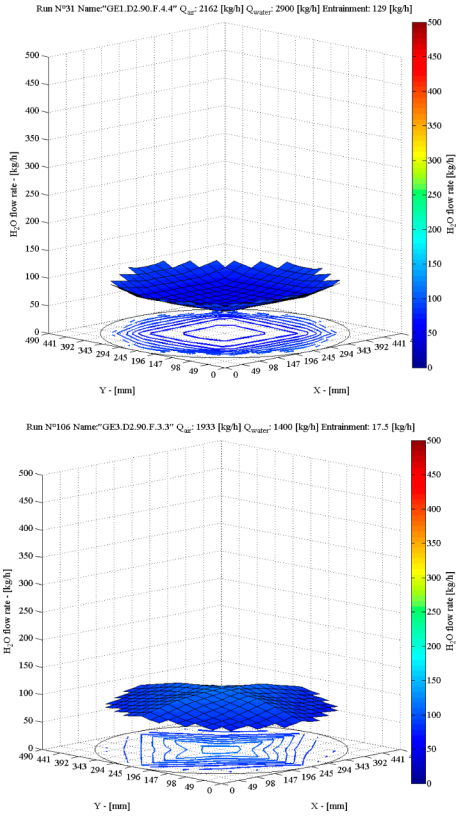

Figure 20. Liquid distribution below the packing with higher water flow rate and different plugging of drip points.

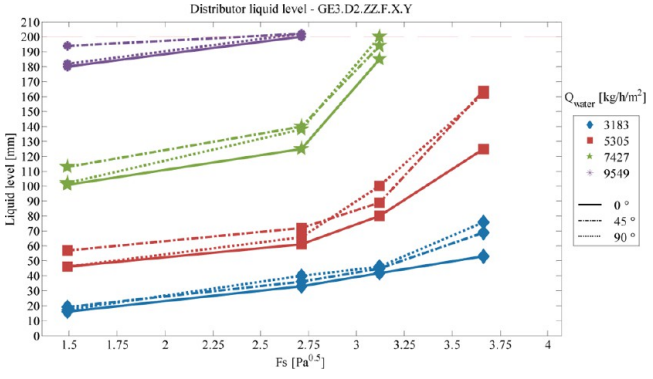

Figure 21. GE3.D2.zz.F.x.y, liquid level on the distributor.

the packing. This allows the gas to reduce its dissipation of kinetic energy while moving toward the gas risers. This originates maldistribution of the flow inside the packing together with the drastic pressure increase under the distributor that induces the liquid level to increase above it.

The accumulation of liquid at high flow rates is also responsible for entrainment (Figure 25). If B is the minimum riser width and D the distance between the distributor and the packing, the configuration D1 is characterized by a ratio D/B = 1, whereas D2 has D/B = 5. As a preliminary qualitative analysis, it is possible to observe that whenever this ratio is less than or equal to 5, some negative fluid-dynamic problems occur with a consequent increase of entrainment and overflow conditions. As a side effect, a decrease of the packing efficiency has to be expected because of the stream line deviations bypassing a part of the packing. These negative effects are validated by data in Figure 26. The liquid distribution after the packed bed clearly shows a significant maldistribution for the configuration D1, especially for high F_s where the peripheral zone is overwetted while the center is quite dry.

It is interesting to observe now Figure 27, where the experimental maldistribution is reported as a function of the ratio between air and water flow rate (massive flow). It is the only case we have found where the influence of gas flow rate is evident and correlated to the air flow rate.

4.2. Humidification Tests. The last set of experiments is focused on the humidification at the top of the packed column. The humidification of air is a relatively simple way and an important measure to infer the efficiency of the mass transfer with respect to the selected geometries.

The column layout has been partially modified (Figure 28) in order to reduce the effect of the water running out of the packaging. The water collector has been removed. The gas distribution is not anymore affected by the presence of vessels. Accordingly, the instrumentation has been repositioned.

The humidification tests compare GE1.Dz.90.F.x.y.SV with z = 1, 2. Figure 29 shows two different trends of the humidification related to the distributor to packing distance. In the configuration with the distance D1, that is, the minimum one, the profiles show a decrease of the humidification with the air flow rate increase. This is due to the phenomena already discussed in the section devoted to the effect of distributor to packing distance, i.e., to the maldistribution of air along the packing related to the need of the air streamlines to reach the risers with a convenient orientation. Experimental data for distance D2, which has been indicated as the optimum one, emphasize the dependence on the water flow rate (assigned the air flow rate, the larger water flow rate, the higher humidification) as well as on the air flow rate (the larger the air flow rate, the larger the humidification). The dependence on

GE3.D2.**00**.F.1.4

Vessel n°	m³/h	Av. m³/h
1	0.120	0.110
2	0.100	
3	0.110	**Mf**
4	0.100	**0.030**
5	0.130	
6	0.120	
7	0.110	
8	0.110	
9	0.130	

GE3.D2.**45**.F.1.4

Vessel n°	m³/h	Av. m³/h
1	0.120	0.114
2	0.112	
3	0.120	**Mf**
4	0.120	**0.017**
5	0.120	
6	0.106	
7	0.112	
8	0.112	
9	0.106	

GE3.D2.**90**.F.1.4

Vessel n°	m³/h	Av. m³/h
1	0.106	0.122
2	0.120	
3	0.112	**Mf**
4	0.112	**0.033**
5	0.112	
6	0.128	
7	0.138	
8	0.128	
9	0.138	

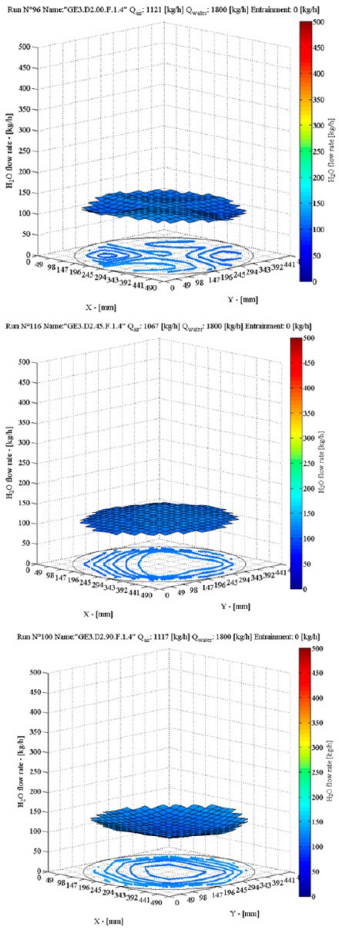

GE3.D2.**00**.F.4.1

Vessel n°	m³/h	Av. m³/h
1	0.004	0.021
2	0.016	
3	0.021	**Mf**
4	0.011	**0.201**
5	0.016	
6	0.045	
7	0.018	
8	0.036	
9	0.190	

GE3.D2.**45**.F.4.1

Vessel n°	m³/h	Av. m³/h
1	0.004	0.028
2	0.019	
3	0.016	**Mf**
4	0.014	**0.208**
5	0.017	
6	0.048	
7	0.042	
8	0.051	
9	0.042	

GE3.D2.**90**.F.4.1

Vessel n°	m³/h	Av. m³/h
1	0.001	0.024
2	0.015	
3	0.015	**Mf**
4	0.016	**0.210**
5	0.015	
6	0.045	
7	0.036	
8	0.042	
9	0.036	

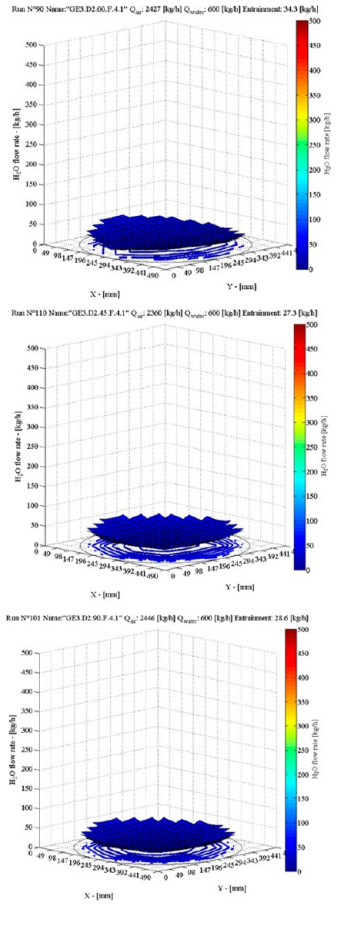

Figure 22. Liquid distribution below the packing as a function of twist angle and air and water flow rate.

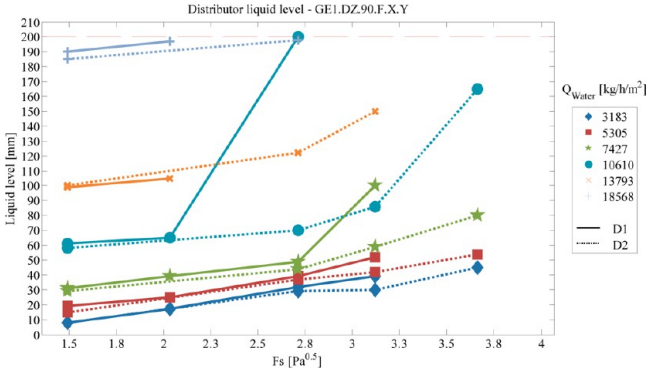

Figure 23. GE1.Dz.90.F.x.y, liquid level on the distributor.

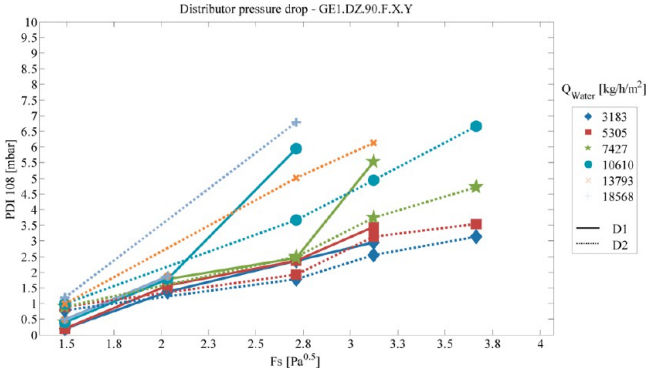

Figure 24. GE1.Dz.90.F.x.y, pressure drops on the distributor.

the liquid load is easy to explain since the larger content of water in the structured packing, the larger the mass transfer. The increase of the air humidification is due to the well-distribution of the air along the column, which is mainly related to the space availability between the distributor and the packing. Such behavior has the effect of exploiting at best the potentialities of the overall packed bed, without any shadow region at the top due to the convenient orientation of the air streamlines within the packing. The humidification tests show that in configuration D2, even if a nonoptimal liquid distribution is always assured (as demonstrated in the previous figures), the air humidification is assured and a good exchange among phases is performed. This is due to the fact that no dry areas are present on the packing and also to the contribution to the mass transfer given by the raining effect in the sections where the packing is absent.

5. ENTRAINMENT

The following part of the paper will be devoted to the investigation of nonconventional situations such as the entrainment phenomenon and the loading condition.

Liquid can be entrained by the gas. A portion of the liquid phase fed to the column (i.e., the one coming from the condenser) is entrained directly toward the top of the column, without entering the packing. The overall efficiency of the

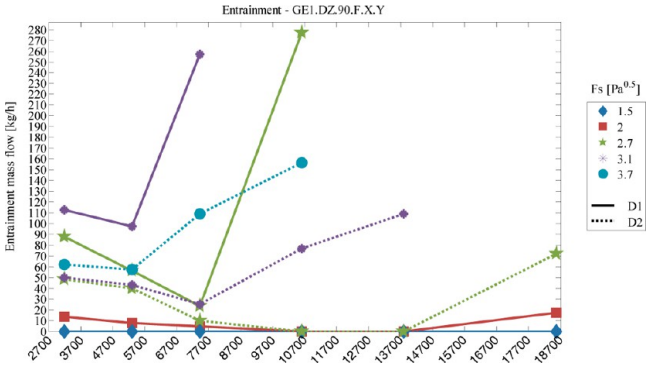

Figure 25. GE1.Dz.90.F.x.y, entrainment flow rate.

column is unavoidably reduced since a smaller mass transfer takes place in the structured packing.

Considering the air/water system,[12,20,23,28,30,32] the entrainment problem is not so relevant since the outlet air at the top of the column has an already high humidity due to the entrained water. On the other hand, in more sophisticated industrial systems, such as the cryogenic towers for air fractionation,[35,36] if in the low-pressure column there is a too high oxygen concentration, for instance larger than the 0.5%, large economic losses are expected since the final product is not pure.

Some of the reasons for the phenomenon have been already discussed in the literature,[28,37−48] such as the liquid outflow instability, the generation of droplets, the high velocity of the liquid outflow, and its splashing on the packing, and the excess of air flow-rate with consequent loading and flooding of the packing or the liquid distributor as well.

The theory of falling jets and films, the studies on the droplet generation, and the splashing phenomena all together play a fundamental role for the generation of the entrainment. The liquid jets leaving the drip points of the distributor deck can preserve their stability until they achieve the packing, but if the distance from the origin is sufficient, they can also break forming drops (Plateau−Rayleigh instability).[47,48] These drops can subsequently generate subdroplets by splashing against the packing, and finally the smallest droplets can be entrained. Other phenomena can give a relevant contribution. For instance, when the gas flow rate rises, the film laying on the packing surface can flow in the gravity direction or follow the gas on its free surface with the consequent generation of waves and, next, droplets and entrainment.

More difficult is the characterization of phenomena governing the droplet/packing surface interactions. They have been investigated by many authors, and several reviews of the subject are available.[37,40,42] The theoretical studies of droplet and surface interaction started with the analysis of the impact of a single droplet. Roisman et al.[44] proposed a theory for droplet on a dry surface where the splash depends on the density and surface tension of the liquid, the droplet diameter, and the impact velocity. The theory was subsequently extended to the case of wet surfaces, to two droplets[43,45] and, next, to multiple droplets with many numerical solutions of the problem.[41,46]

The fluid flow associated with impinging droplets is rather complicated and not yet fully understood. Various phenomena can occur when a droplet impacts a surface, and the outcome depends on the droplet and surface properties. As reported by Sikalo and Ganic,[45] the number of independent parameters governing the process can be reduced to a set of dimensionless groups, particularly on Weber number. Other studies proposed more detailed characterization of the droplet splashing[38,39] by separating the effects of kinetic energy and viscous dissipation.

Unfortunately, if the aforementioned phenomena have been singularly investigated, their interactions and the relationships among the entrainment, the loading, and the flooding conditions are not yet well understood. So now the aim is to provide a comprehensive interpretation of dedicated experimental data sets by means of a phenomenological discussion.

6. WEEPING (OR DRIPPING)

As said before, the instability of the liquid outflow from the distributor desk generates entrainment, influencing the packing efficiency.[4,10,49]

The weeping tests are aimed at investigating what is the maximum distributor to packing distance for having a stable film. Two different geometries have been selected for the weeping tests: with 36 drip points (in the following GE1) and 18 drip points (in the following GE3). Moreover, to allow the reproduction of the tests, it is worth saying that the preferred twist angle is 90°, the distributor to packing distance is 26 cm (D2), and there is a null specific air flow rate. With a specific liquid flow rate of 7950 kg/h/m^2 (1500 kg/h), the minimum liquid level for the distributor is 30 mm. The weeping tests have been performed directly within the packed column with zero air load and different water loads. Measurements are made by means of an internal dedicated flange.

The undisturbed length of the jet has been derived by Rayleigh and reported, for instance, by Levich.[50] The length prior to breakup depends on the outflow velocity v_L, the density ρ_L, the liquid surface tension σ_L, and the drip point diameter D:

$$L = 8.46 \cdot \sqrt{\rho_L D^3/\sigma_L} \cdot v_L \tag{3}$$

The proposed relation is not affected by the presence of a countercurrent gas. Assigning an average predefined liquid load to the distributor, the outflow velocity is evaluated from

$$v_L = C_c\sqrt{2gh_L} \tag{4}$$

where C_C is the outflow coefficient, h_L is the liquid level (in m), and v_L is the outflow velocity (in m/s). The outflow coefficient has a value of 0.6. The liquid level in the distributor is also a function of the gas flow rate. The pressure drop (in Pa·H_2O cm) can be evaluated with the following expression:

$$\Delta P_{gas,distributor} = \rho_G\left(\frac{W_{gas}}{S_{column}}\right)^2 \cdot \left[\frac{3}{\varepsilon^2} + \frac{(1-\varepsilon)^2}{2}\right] \tag{5}$$

where W_{gas} is the volumetric gas flow rate, S_{column} is the column section, and ε is the fraction of the column section devoted to the risers. The total liquid level to be used in eq 4 is solely related to the liquid velocity corresponding to the liquid volumetric flow rate divided for the total drip points section.

The undisturbed liquid jet length is reported in Figure 30 as a function of the liquid level in the distributor in the case of zero gas flow rate. It is possible to observe that an adequate reduction of the operational range can ensure the stability in the outflowing liquid film. Nevertheless, once a certain load is defined, the constraint of minimum liquid level on the distributor must be satisfied (vertical line). The horizontal lines define the distributor to packing distances adopted in the weeping tests. Too small distances do not have enough space to generate droplets, but as already demonstrated, they generate

GE1.**D1**.90.F3.1

Vessel n°	m³/h	Av. m³/h
1	0.007	0.028
2	0.011	
3	0.012	Mf
4	0.011	0.260
5	0.012	
6	0.040	
7	0.045	
8	0.067	
9	0.047	

GE1.**D2**.90.F3.1

Vessel n°	m³/h	Av. m³/h
1	0.014	0.031
2	0.033	
3	0.031	Mf
4	0.034	0.08
5	0.029	
6	0.037	
7	0.041	
8	0.029	
9	0.032	

GE1.**D1**.90.F3.2

Vessel n°	m³/h	Av. m³/h
1	0.009	0.031
2	0.018	
3	0.018	Mf
4	0.019	0.187
5	0.017	
6	0.045	
7	0.050	
8	0.046	
9	0.051	

GE1.**D2**.90.F3.2

Vessel n°	m³/h	Av. m³/h
1	0.016	0.047
2	0.047	
3	0.052	Mf
4	0.053	0.085
5	0.048	
6	0.047	
7	0.055	
8	0.046	
9	0.054	

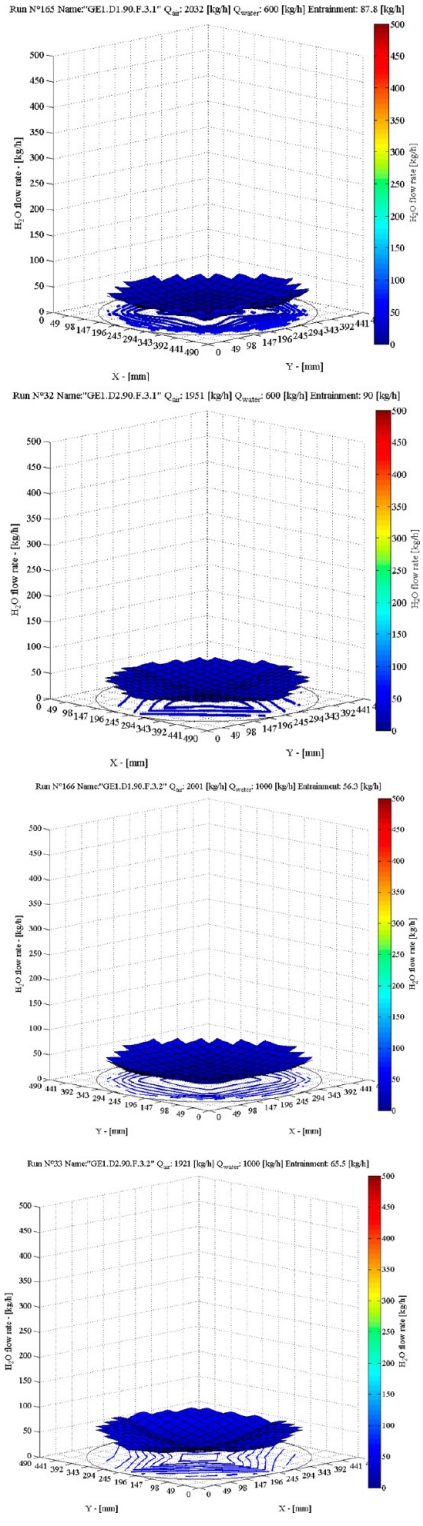

Figure 26. Liquid distribution below the packing for distance D1 and D2.

serious problems for the gas that is rising in the column and are not taken into consideration.

Figure 31 shows the liquid jet obtained in different water. In Figure 31a, it is worth noticing that the distributor is not fully operating since, the liquid level being smaller than the limit of 30 mm (normal conditions), some drip points are not irrigated (see on the top-right of the figure).

Figure 31b shows the formation of the droplet; nevertheless, the instability appears several centimeters above. Figure 31c underlines that the outflowing liquid is still influenced by the limit condition of a liquid level approaching 30 mm; actually, the jet generates droplets. Figure 31d shows the liquid under the same conditions of the previous point. In this case, the jet seems to be more stable. In Figure 31e, the outflow is more and more stable. In Figure 31f, the liquid jet is completely stable.

To work properly, the liquid distributor must be placed on a horizontal support. The solders, the punching, the installation

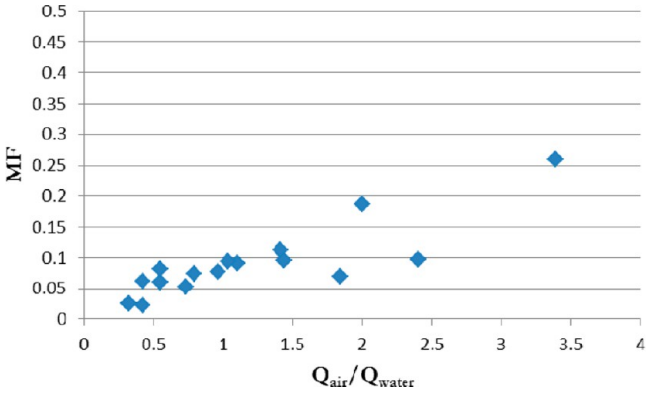

Figure 27. Maldistribution versus air/water mass flow rate.

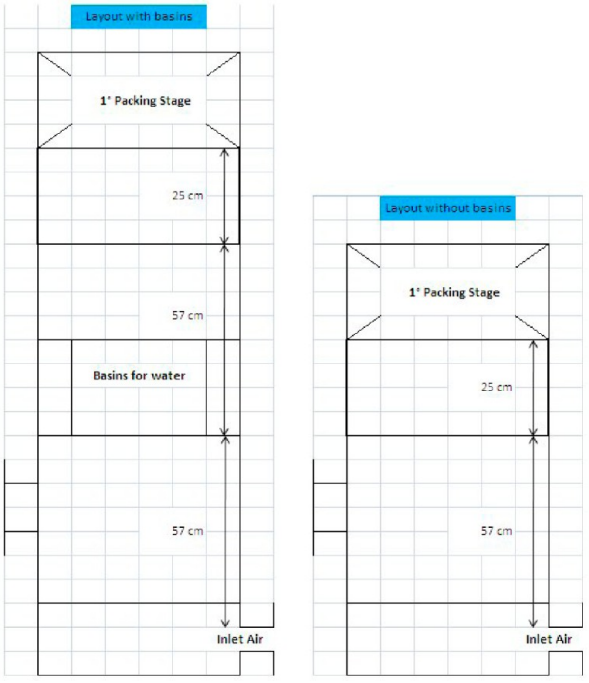

Figure 28. Packed column layout modification for reliable humidity measures. This layout is identified with the suffix SV in the geometry code.

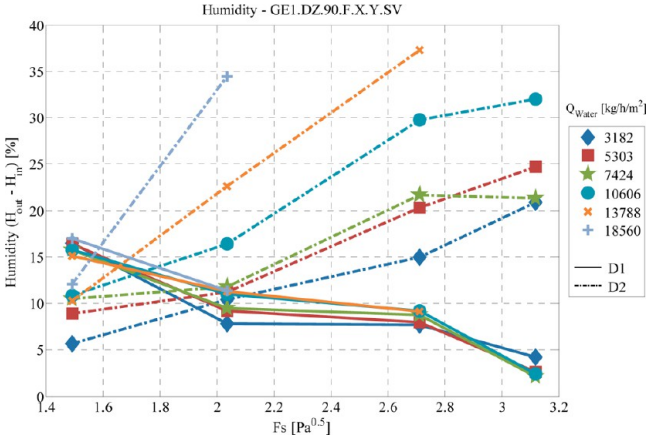

Figure 29. GE1.Dz.90.F.x.y.SV with z = 1, 2; humidity trend.

of the risers, and especially the weight of the same distributor can lead to out-of-plane configurations.

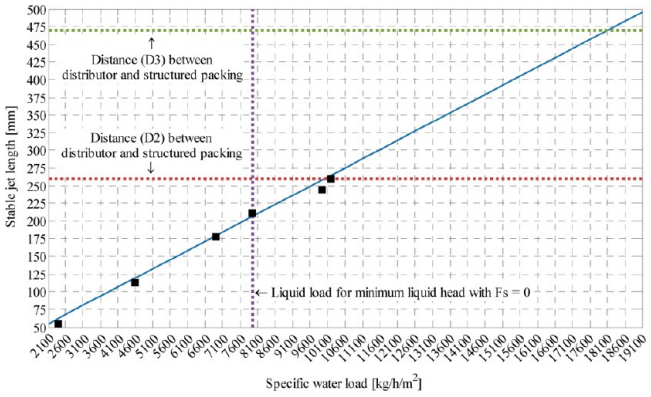

Figure 30. Stability (limit of film length): comparison of experimental data with eq 3.

Supports are usually installed for the industrial distributors to prevent these deformations. The distributor used in the experiments does not require these construction devices since the column internal diameter only is 490 mm, but it was decided to insert the support to simulate at best the industrial cases. The mechanical support of the liquid distributor needs to resist some hundreds of kilograms for high loads; thus, it consists of stainless steel tubular bars with a rectangular cross section. If the bars are installed too close to the drip points, they can intercept the liquid jet, leading to earlier droplet generation. Finally, Figure 32 relates to a specific liquid flow rate of 4000 kg/h/m^2. The liquid jets are well-developed for the first 8 cm, but the two jets closer to the support structure are subject to a wall, inducing the earlier generation of droplet, and, consequently, an increase of the entrainment I.

7. SPLASHING EFFECT ON THE STRUCTURED PACKING

As demonstrated above, the liquid jet can be continuous or scattered in droplets. In the latter case, it is necessary to assess how the single droplet impacts and what happens, once it has achieved the wetted, oblique, and waved surface of the structured packing. The dynamics of the impact on the surface depends on the drop diameter, its terminal velocity, the physical characteristic of the fluid (viscosity, density, surface tension), and the surface roughness. In order to have the splash of the drop, the Weber number ($\rho_L v_{rel}^2 D/\sigma$) has to overcome at least a value of 80. Below this limit, the drop bounces. Stow and Stainer found that the splash-product diameters are distributed according to a log-normal function, and that the number of droplets produced by a splash increases with surface roughness, impact velocity, and drop size but decreases with a reduction of the surface tension.

Here, the purpose is just to put into light the contribution to entrainment of possible drops splashing over the packing surface. An estimation of the number of subdroplets generated after the splashing is obtained through the experiments to evaluate their volumes and, with a momentum balance, the fraction entrained by the specific air load.

The kinetic energy of the falling droplet is a function of the liquid properties, of the velocity, and of the shape. The kinetic energy is almost totally dissipated in the impact on the packing surface. This dissipation is mainly due to the viscous and inertial frictions. The remaining energy is transformed into kinetic and surface energy of the subdroplets, which are generated in the impact. The energy dissipation is evaluated by

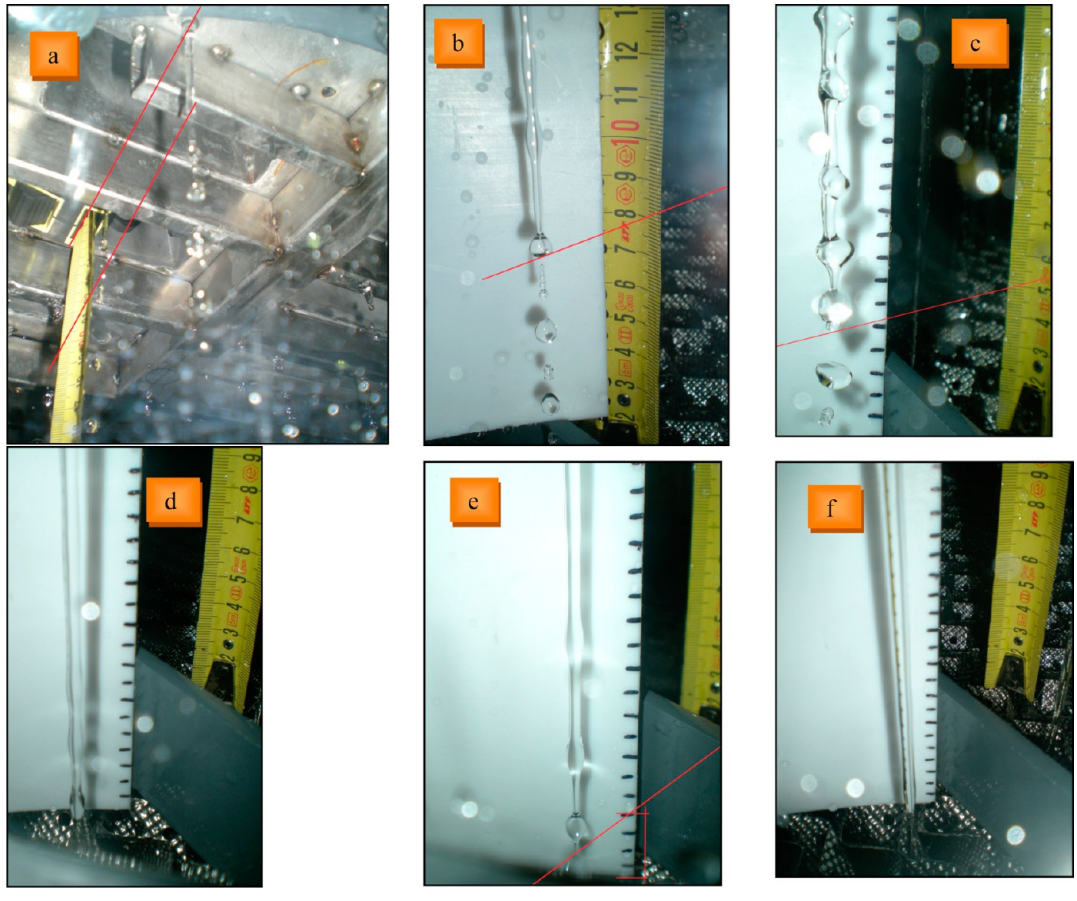

Figure 31. Jet stability at different water loads. (a) 2100 kg/h/m^2; (b) 6900 kg/h/m^2; (c) 7960 kg/h/m^2; (d) 7960 kg/h/m^2; (e) 9950 kg/h/m^2; (f) 10100 kg/h/m^2.

Figure 32. Stainless steel support for the industrial distributors.

means of a nondimensional parameter, called breaking efficiency, which is given by the ratio of the value 12 (this value is an average critical value of the *We* number of the drops after their formation) and the *We* number:

$$\eta = \frac{12}{We} = \frac{12\sigma}{\rho_L v_{rel}^2 D_{sub\text{-}droplet}} \quad (5)$$

where σ is the interfacial tension of liquid, ρ_L the liquid density, $D_{subdroplet}$ diameter of the formed subdroplet, and v_{rel} is the gas–liquid relative velocity. This parameter allows evaluating the total volume of the subdroplets that are formed after the impact.

Regarding the diameter of the subdroplets, some specific tests have been performed to identify their average size. Thanks to a relatively high resolution photo camera (250 fps), it has been possible to obtain a sequence of images of the droplet splashing on a metallic surface very similar to the one of the structured packing (see Figure 33). The sequence shows that a set of subdroplets are originated from the splashing of a single droplet. The subdroplets separate from the crown generated by the impact at the photogram (c). It is possible to count the subdroplets. After many tests with different mother droplets, the average of subdroplets generated has converged to 15.7. Thus, the average diameter of the subdroplet is 0.7 mm.

The structured packing Mellapak 250.Y does not have a flat surface, but it is characterized by layers of metallic sheets at 45°. Hence, the same analysis has been performed on a stainless steel surface at 45°, and the photograms are reported in Figure 34. A first important difference with respect to the previous case is that the crown originated by the impact is deformed. The angle of inclination of the metallic surface deflects the droplet toward the slope, and the kinetic dissipation is less drastic since the droplet tends to slide on the wetted oblique surface. The number of subdroplets is 14.1 in this case, with a diameter of 0.6 mm.

Using the experimental diameter, it is possible to provide a reasonable estimation of the subdroplets formed by the splashing. It is therefore possible to estimate the efficiency of breaking of the droplet by evaluating the relative velocities between the fluids in the column under the different operating

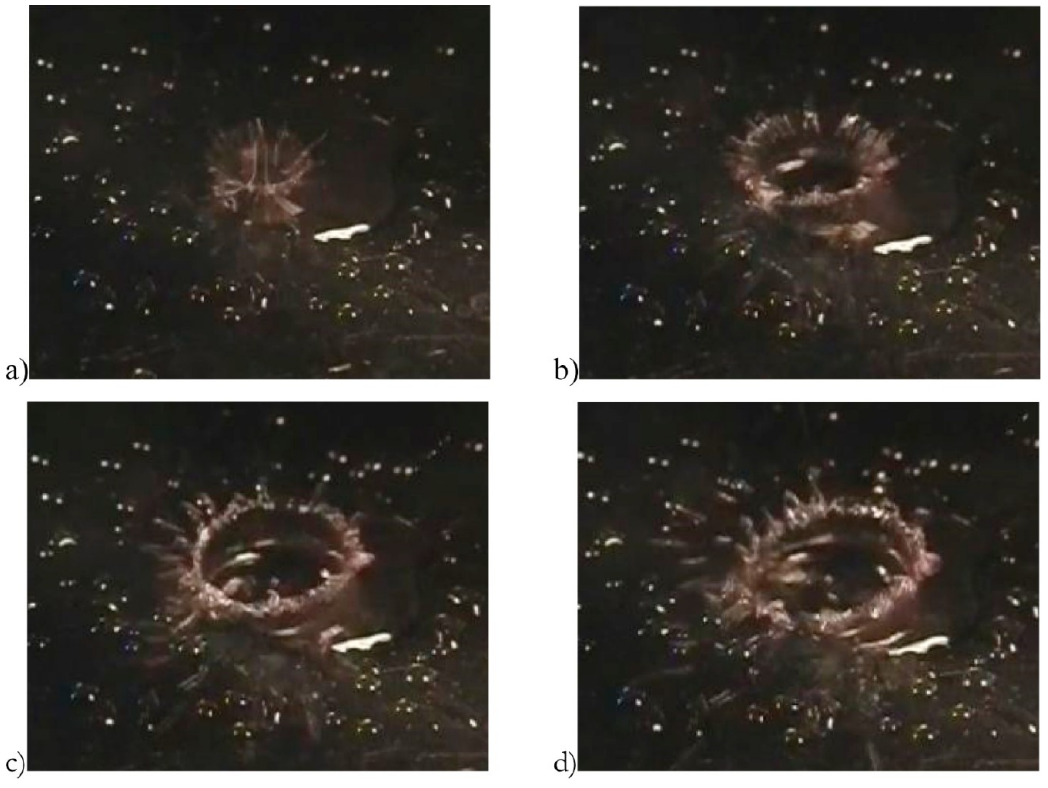

Figure 33. Droplet splashing sequence (horizontal surface).

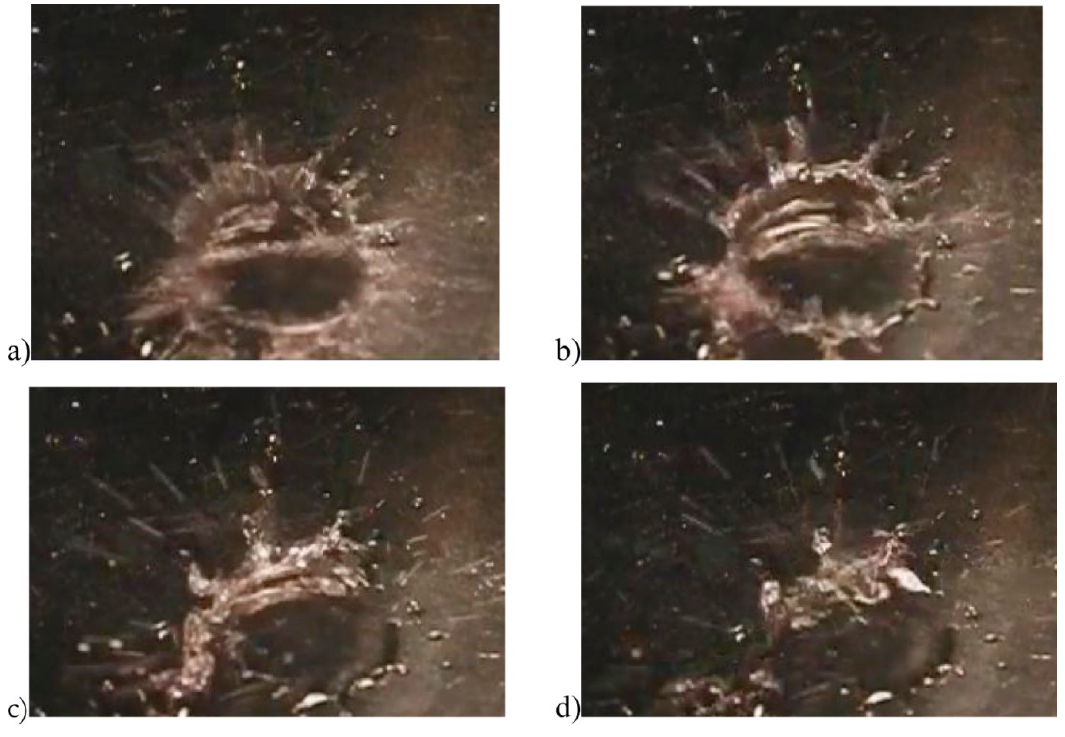

Figure 34. Droplet splashing sequence (45° surface).

conditions. The efficiency assumes, in the present study, the following values:

$$0.01 < \eta < 0.1 \tag{6}$$

The average diameter of the droplets can be calculated for several values of the efficiency by assuming that 14 droplets are forming (this is the case of Mellapack 250Y or other packings having the corrugations inclined 45° with respect to the horizontal plane and with an air–water system):

$$D_{\text{sub-droplet}} = \left(\frac{6}{\pi}\frac{V_{\text{drop}}\cdot\eta}{14}\right)^{1/3} \tag{7}$$

where V_{drop} is the volume of splashing drop.

To check if the subdroplets are entrained by the air load, a momentum balance is performed, by supposing a spherical shape:

- Buoyancy force:

$$\dot{F}_G = \rho_{air} V_{droplet} g \tag{8}$$

- Gravity force:

$$\vec{F}_P = \rho_{droplet} V_{droplet} g \tag{9}$$

- Impact force

$$\vec{F}_T = \frac{1}{2}\rho_{air} C_D v_{rel}^2 \frac{\pi \cdot D_{droplet}^2}{4} \tag{10}$$

where C_D is the drag coefficient taking into account also drop deformation, deduced by using the theory introduced by Bozzano et al.[51]

The entrainment condition is, obviously

$$\vec{F}_G + \vec{F}_T > \vec{F}_P \tag{11}$$

8. EFFECT ON ENTRAINMENT OF LOADING CONDITION OF THE STRUCTURED PACKING

As stated in the literature, the loading condition corresponds to about the null velocity at the gas–liquid interface. To assess if a correlation between the loading conditions, which are the most favorable for the mass transfer, and the entrainment phenomenon exists, it is necessary to identify which operating conditions generate the loading (Figure 35). The gas flow rate

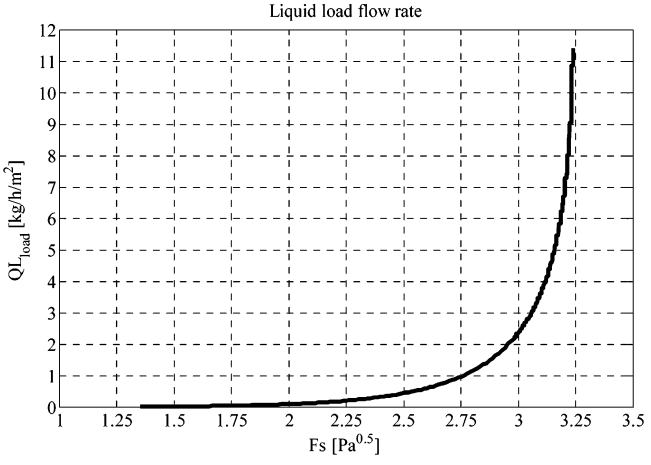

Figure 35. Liquid loading with respect to gas flow rate.

needed to determine the loading phenomenon increases together with the liquid load. The liquid load that corresponds to the loading slowly increases for small gas flow rates, whereas it has an exponential increase for large gas flow rates. It is linear with respect to the specific gas load up to $F_s = 2.25$, whereas the exponential trend with large F_s is related to the shear stresses generated by the gas flow rate. The curve has been calculated by using the model of Bozzano and co-workers.[31]

While the liquid load increases, the average thickness of the liquid film within the packing increases too, and the holdup rises. Beyond certain liquid and gas loads, the only extreme condition is the flooding, where an exponential increase of pressure drops, efficiency losses for the mass transfer (due to the formation of prevalent channels for liquid flows), and increase of the entrainment are observed.

To detect the operating regime of the packed column, for instance, close to the loading or over the entrainment, it is necessary to compare the flow rate entering the column with respect to the calculated loading condition. Considering some cases shown in Figures 36–38, note that with an increasing

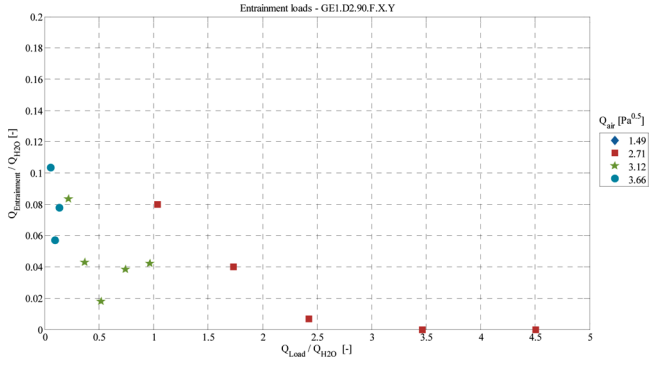

Figure 36. Entrainment flow rate for the geometry GE3 and twist angle 90°.

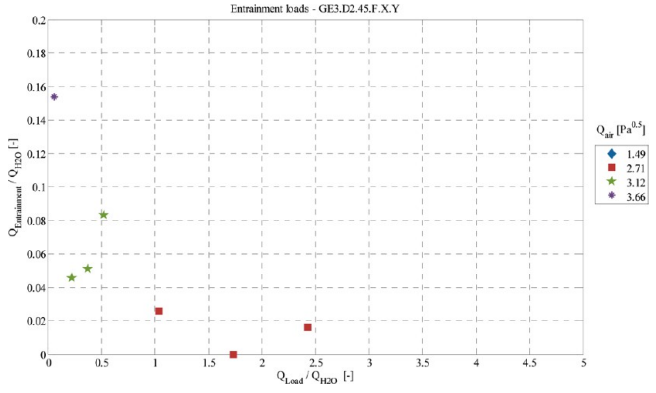

Figure 37. Entrainment flow rate for the geometry GE3 and twist angle 45°.

ratio of loading specific flow rate and liquid specific inlet flow rate, the entrainment approaches zero. Changing the geometry of the liquid distributor, for instance the twist angle, the result is the same since an increase in the liquid flow rate leads to

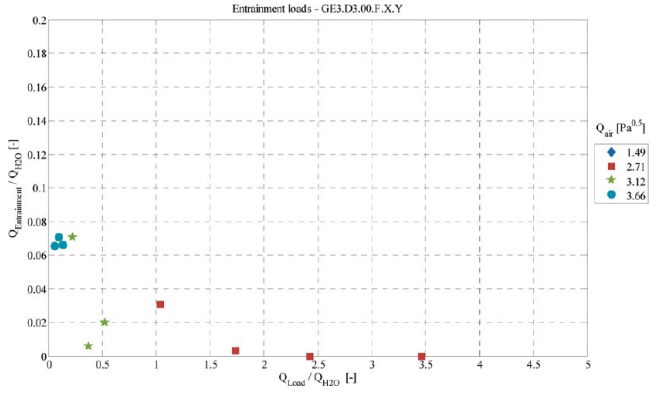

Figure 38. Entrainment flow rate for the geometry GE3 and twist angle 0°.

relevant entrainment only if the ratio is close to 1 or higher (beyond the loading condition).

In the series of tests with F_s = 1.49, due to the low gas flow rate, the entrainment is always prevented (Q_{load}/Q_{H_2O} > 10). Figures 36−38 show the entrainment for different twist angles (90° to 45° and to 0°). Several phenomena can be deduced with respect to the liquid flow rate:

1. The fraction of liquid entrained is almost always zero for Q_{load}/Q_{H_2O} > 1. When the entrainment is present, it is due to the low liquid flow rate, which cannot ensure a continuous outflowing jet with consequent weeping, droplet generation, and, next, entrainment formation.

2. With an assigned gas flow rate, there is a quasi-quadratic relationship that joins the entrainment flow rate and the liquid flow rate. In fact, at low water flow rates, the entrainment is mainly due to the maldistribution for weeping and droplet generation. Conversely, the outflowing jet is more stable with larger liquid flow rates, and the droplet formation is reduced or absent. At last, the liquid entrained increases beyond the loading conditions.

3. With large gas flow rates (F_s > 3), the inlet liquid flow rates are always sufficient to lead to the loading condition. The relationship between the loading conditions (and the more critical flooding conditions) and the entrainmentIt is definitely evident. To quantify the effects of liquid flow rates larger than the loading flow rates, it is necessary to calculate the fraction of liquid holdup within the structured packing under the operating conditions.

9. CONCLUSIONS

This work, together with the companion paper, has the purpose to contribute to the current literature on the design criteria for fluid distributors coupled with structured packing systems. The sole experimental campaign required several months on the pilot plant with dedicated human resources from both the Politecnico di Milano and SIAD Macchine Impianti. The activity is resulted in the collection of a large amount of data (184 tests), which allowed a deeper process understanding and detailed discussions.

Different geometries of the liquid distributor with respect to the packing have been performed to assess the interactions with the underlying packing. The highlights can be summarized as follows:

- The selected drip points distributor has demonstrated an optimal wetting of the structured packing. When the gas flow rate is zero or however far from the loading conditions, the liquid distribution is particularly uniform. Whenever F_s increases and the system approaches the loading conditions, the distribution is somehow compromised and the column efficiency declines.
- The variation of the twist angle does not have a relevant impact on the distribution efficiency of the liquid on the structured packing. Conversely, significant phenomena are present for the gas fluxes: if the risers are oriented as the layers of the structured packing, the turbulence generated by the air flow rates is reduced with a consequent reduction of the pressure drops across the fluid distributor and of the entrainment. The riser disposition should cover the maximum surface so as to decrease the air contraction between the packing and the distributor (in our plant it was covering 30% of the distributor).
- The distributor to packing distance is a crucial parameter with direct effects on the gas and liquid distribution. Whenever the distributor is installed too close to the packing, the gas fluxes must strongly deflect their path in a reduced space for entering the risers. It causes a redirection of the gas streamlines already within the packing, generating a kind of bypass zone where the liquid is favored to pass in. There is a consequent decrease of the mass transfer efficiency and a liquid maldistribution along a part of the packing. In this case a direct correlation between air flow increase and maldistribution increase has been highlighted. The minimum distance between distributor and packing has to be such that the ration between the this distance and the risers minimum width is equal to 5. Nevertheless, an installation of the distributor too far from the packing worsens the hydraulic behavior for the entrainment of the droplets on top of the packing, although the gas fluxes are free to move and enter the risers without relevant pressure drops. Equations 1−5 and the model that describes the droplet generation from a liquid jet, eqs 6−11, and their consequent entrainment allow one to evaluate the optimal distance between the packing and the liquid distributor.
- The stainless steel support for the packing must be soldered in order to prevent the contact of the liquid jet outflowing drip points with the supporting bars. Actually, if the liquid jet deviates from its vertical path, unavoidably earlier droplet generation can take place and, with their splashing, produce subdroplets and, consequently, entrainment.
- The liquid and gas flow rates play a fundamental role in the liquid entrainment. Large gas flow rates lead to entrainment phenomena also into the structured packing when loading conditions are approached.
- The losses in the column efficiency are therefore due to the selected packing. An increase in the gas flow rate generates a crown effect in the packing wetting with a kind of bypass in the central zones and a large flow of liquid in the peripheral zones. Such bad contacting reduces the mass transfer although the geometrical configuration works well from a hydraulic viewpoint.

Finally, the set of reasons responsible for generating fluid-dynamic problems in the packed column and liquid distributor have been investigated. A better understanding is the basis for the improvement of plant efficiency and the reduction of the installation and variable costs. The present paper can be a starting point toward further investigation of interactions between the liquid distributor and the structured packing when their geometries are changing. Moreover, also the effect of fluids with different interfacial tension should be investigated.

AUTHOR INFORMATION

Corresponding Author

*Phone: +39 (0)2 2399 3094. Fax: +39 (0)2 7063 8173. E-mail: giulia.bozzano@polimi.it.

Notes

The authors declare no competing financial interest.

REFERENCES

(1) Lockett, M. J.; Billingham, J. F. The Effect of Maldistribution on Separation in Packed Distillation Columns. *Trans. IChemE, Part A* **2003**, *81*, 131−135.

(2) Albright, M. A. Packed Tower Distributors Tested. *Hydrocarbon Process.* **1984**, 173.

(3) Bonilla, J. A. Don't Neglect Liquid Distributors. *Chem. Eng. Prog.* **1993**, *89*, 47.

(4) Spekuljak, Z.; Monella, H. Fluid distributors for structured packing columns. Annual AIChE Meeting, Miami, Florida, November 1998.
(5) Marchot, P.; Toye, D.; Crine, M.; Pelsser, A.-M.; L'Homme, G. Investigation of liquid maldistribution in Packed columns by X-ray tomography. *Trans. IChemE, Part A* **1999**, *77*, 511−518.
(6) Hoek, P. J. Large and Small Scale Liquid Maldistribution in a Packed Column. Ph.D. Thesis 1983, Technische Hogeschool Delft, Delft, The Netherlands.
(7) Hoek, P. J.; Wesselingh, H.; Zuiderweg, F. J. Small scale and large scale liquid maldistribution in packed columns. *Chem. Eng. Res. Des.* **1986**, *64*, 431−449.
(8) Ter Veer, K. J. R.; Van Der Klooster, H. W.; Drinkenburg, A. A. H. The Influence of the Initial Liquid Distribution on the Efficiency of a Packed column. *Chem. Eng. Sci.* **1980**, *35*, 761−762.
(9) Pizzo, S. M.; Moraes, D.; Fernandes, F. A. N.; Kobayasi, M. S.; Pazini, R. J. Analysis of Liquid Distribution in a Packed Column on a Pilot Scale. *Ind. Eng. Chem. Res.* **1998**, *37* (7), 2844−2849.
(10) Kouri, R. J.; Sohlo, J. Liquid and gas flow patterns in random packings. *Chem. Eng. J.* **1996**, *61*, 95−105.
(11) Kouri, R. J.; Sohlo, J. Liquid and gas flow patterns in random and structured packings. *IChemE Symp. Ser.* **1987**, *104*, B193.
(12) Ibrahim, A. A. Experimental Study of Liquid Distribution in Packed Column. *J. King Saud Univ., Eng. Sci.* **1998**, *10* (2), 271−284.
(13) Semkov, K. R. Liquid Flow Distribution in Packed Beds by Multipoint Liquid Distributors. *Chem. Eng. Sci.* **1991**, *46* (5−6), 1393−1399.
(14) Sun, C. G.; Yin, F. H.; Afacan, A.; Nandakumar, K.; Chuang, K. T. Modelling and simulation of flow maldistribution in random packed columns with gas-liquid countercurrent flow. *Trans. IChemE, Part A* **2000**, *78*, 378−388.
(15) Scott, A. H. Liquid distribution in packed towers. *Trans. IChemE* **1935**, *13*, 211.
(16) Tour, R. S.; Lerman, F. Unconfined distribution of liquid in tower packing. *Trans. AIChE* **1939**, *35*, 709.
(17) Dutkai, E.; Ruckenstein, E. Liquid distribution in packed columns. *Chem. Eng. Sci.* **1968**, *23*, 1365.
(18) Cihla, Z.; Schmidt, O. A study of the flow of liquid when freely trickling over the packing in a cylindrical tower. *Collect. Czech. Chem. Commun.* **1957**, *22*, 896−907.
(19) Onda, K.; Takeuchi, H.; Maeda, Y.; Takeuchi, N. Liquid distribution in a packed column. *Chem. Eng. Sci.* **1973**, *28*, 1677.
(20) Stikkelman, R. M.; de Graauw, J.; Olujic, Z.; Teeuw, H.; Wesselingh, H. A Study of Gas and Liquid Distribution in Structured Packings. *Chem. Eng. Technol.* **1989**, *12*, 445−449.
(21) Edwards, D. P.; Krishnamurthy, K. R.; Potthoff, R. W. Development of an improved method to quantify maldistribution and its effect on structured packing column performance. *Chem. Eng. Res. Des.* **1999**, *77*, 656−662.
(22) Fitz, C. W., Jr.; King, D. W.; Kunesh, J. G. Controlled liquid maldistribution studies on structured packing. *Trans. IChemE* **1999**, *77*, 482−486.
(23) Olujic, Z.; Van Baak, R.; Haaring, J.; Kaibel, B.; Jansen, H. Liquid distribution properties of conventional and high capacity structured packings. *Chem. Eng. Res. Des.* **2006**, *84* (A10), 867−874.
(24) Spiegel, L. A New Method to Assess Liquid Distributor Quality. *Chem. Eng. Process.* **2006**, *45*, 1011.
(25) Pavlenko, A. N.; Pecherkin, N. I.; Chekhovich, V. Y.; Zhukov, V. E.; Sunder, S. Houghton, Experimental Study of the Effect of Maldistribution at the Structured Packing Inlet on the Freon Mixture Separation Efficiency. *Theor. Found. Chem. Eng.* **2009**, *43*, 1−11.
(26) Alix, P.; Raynal, L. Liquid distribution and liquid hold-up in modern high capacity packings. *Chem. Eng. Res. Des.* **2008**, *86*, 585−591.
(27) Moore, F.; Rukovena, F. Liquid and Gas Distribution in Commercial Packed Towers. *CPP Ed. Eur.* **1987**, 11−15.
(28) Olujic, Z.; Kamerbeek, A. B.; de Graauw, J. A corrugation geometry based model for efficiency of structured distillation packing. *Chem. Eng. Process.* **1999**, *38*, 683−695.
(29) Stikkelman, R. M., Gas and liquid maldistributions in packed columns. Ph.D. Thesis, TU Delft, Delft, The Netherlands, 1989.
(30) Bozzano, G.; Dente, M.; Manenti, F. Fluid Distribution in Packed Beds. Part 1. Literature and Technology Overview. *Ind. Eng. Chem. Res.* **2014**, DOI: 10.1021/ie402137z.
(31) Bozzano, G.; Dente, M.; Corna, P. A Phenomenological Model for Fluid-dynamics Evaluation of Structured Packing Systems. *Chem. Eng. Trans.* **2007**, *12*, 189−194.
(32) Olujic, Z.; Mohamed Ali, A.; Jansens, P. J. Effect of the initial gas maldistribution on the pressure drop of structured packings. *Chem. Eng. Process.* **2004**, *43*, 465−476.
(33) Luyben, W. L. *Process Modeling, simulation and control for chemical engineers*, 2nd ed.; McGraw-Hill: New York, 1990.
(34) Marcandelli, C.; Lamine, A. S.; Bernard, J. R.; Wild, G. Liquid Distribution in Trickle-Bed Reactor. *Oil Gas Sci. Technol.* **2000**, *55* (4), 407−415.
(35) Huang, R.; Zavala, V. M.; Biegler, L. T. Advanced step nonlinear model predictive control for air separation units. *J. Process Control* **2009**, *19* (4), 678−685.
(36) Rodriguez, M.; Diaz, M. S. Dynamic Modelling and Optimization of Cryogenic Systems. *Appl. Thermal Eng.* **2007**, *27*, 1182−1190.
(37) Chandra, S.; Avedisian, C. T. On the collision of a droplet with a solid surface. *Proc. R. Soc. London* **1991**, *A 432*, 13−41.
(38) Cossali, G. E.; Coghe, A.; Marengo, M. The impact of a single drop on a wetted solid surface. *Exp. Fluids* **1997**, *12*, 463−472.
(39) Durickovic, B.; Varland, K. Between Bouncing and Splashing: Water Drops on a Solid Surface. Available at: http://pub.bojand.org/bounce.pdf.
(40) Frohn, A.; Roth, N. *Dynamics of Droplets*; Springer: Berlin, 2000.
(41) Mao, T.; Kuhn, D. C. S.; Tran, H. Spread and rebound of liquid droplets upon impact on flat surfaces. *AIChE J.* **1997**, *43*, 2169−2179.
(42) Rein, M. Phenomena of liquid drop impact on solid and liquid surfaces. *Fluid Dynamics Res.* **1993**, *12*, 61−93.
(43) Roisman, I. V.; Prunet-Foch, B.; Tropea, C.; Vignes-Adler, M. Multiple drop impact onto a dry substrate. *J. Colloid Interface Sci.* **2002**, *256*, 396−410.
(44) Roisman, I. V.; Rioboo, R.; Tropea, C. Normal impact of a liquid drop on a dry surface: model for spreading and receding. *Proc. R. Soc. London* **2002**, *A458*, 1411−1430.
(45) Sikalo, S.; Ganic, E. N. Phenomena of droplet−surface interactions. *Exp. Therm. Fluid Sci.* **2006**, *31*, 97−110.
(46) Sikalo, S.; Wilhelm, H.-D.; Roisman, I. V.; Jakirlic, S.; Tropea, C. Dynamic contact angle of spreading droplets: experiments and simulations. *Phys. Fluids* **2005**, *17*, 062103.
(47) Srolovitz, D. J.; Safran, S. A. Capillary instabilities in thin films. *J. Appl. Phys.* **1986**, *60*, 247−260.
(48) Yu, H. H.; Suo, Z. An axisymmetric model of pore-grain boundary separation. *J. Mech. Phys. Solids* **1999**, *47*, 1131−1155.
(49) Petrova, T.; Semkov, K.; Dodev, C. Mathematical modeling of gas distribution in packed columns. *Chem. Eng. Process.* **2003**, *42*, 931−937.
(50) Levich, V. *Physicochemical Hydrodynamics*, Prentice-Hall International Series; Amudson, N. R., Ed.; Prentice-Hall: Englewood Cliffs, NJ, 1962.
(51) Bozzano, G.; Dente, M. Single bubble and drop motion modeling. *Chem. Eng. Trans.* **2009**, *17*, 567−572.